

Structural Phase Transitions in EuC_2

Derk Wandner,[†] Pascal Link,[†] Oliver Heyer,[‡] John Mydosh,[‡] Mahmoud A. Ahmida,[‡] Mohsen M. Abd-Elmeguid,[‡] Manfred Speldrich,[§] Heiko Lueken,[§] and Uwe Ruschewitz^{*†}

[†]*Department of Chemistry, University of Cologne, Greinstrasse 6, D-50939 Cologne, Germany,*

[‡]*Institute of Physics 2, University of Cologne, Zùlpicher Strasse 77, D-50937 Cologne, Germany, and*

[§]*Institute of Inorganic Chemistry, RWTH Aachen University, Landoltweg 1, D-52074 Aachen, Germany*

Received October 6, 2009

Pure EuC_2 , free of EuO impurities, was obtained by the reaction of elemental europium with graphite at 1673 K. By means of synchrotron powder diffraction experiments, the structural behavior was investigated in the temperature range from 10 to 1073 K. In contrast to former results, EuC_2 crystallizes in the ThC_2 type structure ($C2/c$, $Z = 4$) at room temperature. A tetragonal modification ($I4/mmm$, $Z = 2$) is only observed in a very small temperature range just below the transition to a cubic high-temperature modification ($Fm\bar{3}m$, $Z = 4$) at 648 K. DTA/TG investigations confirm these results. According to Raman spectroscopy, EuC_2 contains C_2^{2-} ions ($\tilde{\nu}(\text{C}\equiv\text{C}) = 1837 \text{ cm}^{-1}$). The divalent character of Eu is confirmed by the results of magnetic susceptibility measurements and ^{151}Eu Mössbauer spectroscopy. In these measurements a transition to a ferromagnetic state with $T_C = 15 \text{ K}$ is observed, which is in reasonable agreement with literature data. Above T_C EuC_2 is a semiconductor according to measurements of the electric resistivity vs temperature, again in contrast to former results. Around T_C a sharp maximum of the electric resistivity vs temperature curve was observed, which collapses on applying external magnetic fields. The observed CMR effect (colossal magnetoresistance) is much stronger than that reported for other EuC_2 samples in the literature. These investigations explicitly show the influence of sample purity on the physical and even structural properties of EuC_2 .

Introduction

Rare-earth metals (RE) form carbides with different carbon contents. The rare-earth metal carbide with the highest carbon contents has the general formula REC_2 and contains C_2 dumbbells. Isostructural compounds are found for alkaline-earth metals with CaC_2 being the most prominent example.^{1,2} The latter is a typical colorless ionic compound, which hydrolyzes upon exposure to water releasing acetylene (C_2H_2). Thus, it can be best described as being composed of Ca^{2+} and C_2^{2-} ions with a C–C bond length of approximately 120 pm, typical for a C–C triple bond.³ Rare-earth metal carbides of composition REC_2 exhibit a different behavior. Most of them show metallic luster and metallic conductivity; hydrolysis leads to a complex mixture of different hydrocarbons.⁴ In a simplifying notation they can be described as being composed of RE^{3+} and C_2^{2-} ions: $\text{RE}^{3+}(\text{C}_2^{2-})(\text{e}^-)$. The additional electron is “responsible” for the metallic properties. The C–C bond length is elongated (128 pm in LaC_2),⁵ as the extra electron occupies antibonding

states of the C_2 unit. This very simple picture can be improved by band structure calculations, which are known for alkaline-earth metal carbides⁶ as well as rare-earth metal carbides.⁷

In this context we are interested in EuC_2 and its properties. Due to the tendency of europium to be stable in the divalent state with a half-filled 4f-shell as well as the trivalent state, EuC_2 could be expected to show either “salt-like” behavior (according to $\text{Eu}^{2+}(\text{C}_2^{2-})$) or metallic behavior (according to $\text{Eu}^{3+}(\text{C}_2^{2-})(\text{e}^-)$). The first synthesis of EuC_2 was reported in 1964 by reacting Eu metal and graphite.⁸ According to this work EuC_2 crystallizes in a tetragonal crystal structure. These results could not be repeated in a later work, and a lower symmetry structure was suggested.⁹ As the reported unit-cell volume of EuC_2 is much larger than those of the other RE^{3+} dicarbides, it was concluded that Eu^{2+} ions were present and that the carbide was wholly ionic. ^{151}Eu Mössbauer spectra corroborated these assumptions,¹⁰ although the reported lattice parameters of the sample under investigation differed

*E-mail: Uwe.Ruschewitz@uni-koeln.de.

(1) Atoji, M. *J. Chem. Phys.* **1961**, 35, 1950–1960.

(2) Knapp, M.; Ruschewitz, U. *Chem.—Eur. J.* **2001**, 7, 874–880.

(3) Pauling, L. *The Nature of the Chemical Bond*, 3rd ed.; Cornell University Press: Ithaca, NY, 1960; p 230.

(4) Palenik, G. J.; Warf, J. C. *Inorg. Chem.* **1962**, 1, 345–349.

(5) Atoji, M.; Gschneidner, K., Jr.; Daane, A. H.; Rundle, R. E.; Spedding, F. H. *J. Am. Chem. Soc.* **1958**, 80, 1804–1808.

(6) Long, J. R.; Hoffmann, R.; Meyer, H.-J. *Inorg. Chem.* **1992**, 31, 1734–1740.

(7) Long, J. R.; Halet, J.-F.; Saillard, J.-Y. *New J. Chem.* **1992**, 16, 839–846.

(8) Gebelt, R. E.; Eick, H. A. *Inorg. Chem.* **1964**, 3, 335–337.

(9) Faircloth, R. L.; Flowers, R. H.; Pummery, F. C. W. *J. Inorg. Nucl. Chem.* **1968**, 30, 499–518.

(10) Colquhoun, I.; Greenwood, N. N.; McColm, I. J.; Turner, G. E. *J. Chem. Soc., Dalton Trans.* **1972**, 1337–1341.

largely from those reported earlier.⁸ In the most recent investigation¹¹ of EuC_2 , a sample was synthesized with lattice parameters quite similar to those reported in the first work on EuC_2 .⁸ In this recent work many physical properties of EuC_2 and its solid solutions with LaC_2 and GdC_2 were investigated.¹¹ Some of them are surprising, as, for example, the electrical resistivity of EuC_2 increases with increasing temperature pointing to a metallic behavior. This disagrees with the assumption that EuC_2 contains Eu in the divalent state, for which a semiconducting or insulating behavior is expected. To clarify these issues, we have synthesized and investigated EuC_2 once again. Special attention must be paid to the synthesis to obtain samples of the highest possible purity. With such samples the structural and some of the physical properties could be reinvestigated.

Experimental Section

General Remarks. Due to the high sensitivity of starting materials (europium) and their products to oxygen and moisture, all sample handling was carried out in an inert atmosphere (Ar, 99.999%). Europium pieces were obtained from Chempur (distilled, 99.99%; Total Rare Earth Metals (TREM): min. 99.92%, Eu/TREM: min. 99.995%) and filed to a fine powder in a glovebox (argon atmosphere). Prior to the reaction graphite (Aldrich, 99.9998%) was heated to 1070 K for 48 h in a dynamic vacuum and stored in an argon atmosphere.

Sample Preparation. In a typical experiment 1.415 g of Eu powder (9.30 mmol) and 0.245 g of graphite powder (20.40 mmol) were mixed in a ball mill placed inside a glovebox. A small surplus of graphite was used (Eu/C = 1:2.2) to inhibit the formation of EuO and to account for graphite losses due to a reaction with the container wall. The graphite and Eu containing powder was transferred into a purified Ta ampule, which was sealed in a He atmosphere (800 mbar). The ampule was heated in an argon atmosphere at 1400 °C (heating rate 400 °C/h) for 24 h and cooled at a rate of 100 °C/h. It is possible to decrease the reaction temperature to 1200 °C without changing the physical properties of the sample. In this case the Ta ampule was placed inside a quartz ampule, which was sealed under vacuum. The quartz ampule was heated in air. The resulting powder is black. None of our experiments showed detectable amounts of EuO or any other impurity as confirmed by X-ray powder diffraction (Huber G670, Mo $K\alpha$ radiation). For resistivity measurements and ¹⁵¹Eu Mössbauer spectroscopic investigations, the sample obtained by the procedure described above was pressed to a pellet (\varnothing 5 mm, 15 min at 2000 kg) and sintered at 500 °C for 96 h (heating rate: 100 °C/h; cooling rate: 20 °C/h) with the pellet placed inside a Ta ampule. After sintering the quality of the sample was again checked by XRPD.

Structural Investigations. Synchrotron powder diffraction data were obtained at the powder diffractometer of beamline B2 of the Hamburg synchrotron facility (HASYLAB, Germany) using the following setups: (i) STOE capillary furnace for high-temperature investigations (298–993 K), position sensitive imaging plate detector system (OBI¹²), $\lambda = 49.9604$ pm; (ii) a closed-cycle He cryostat for low-temperature investigations (10–290 K), position sensitive imaging plate detector system (OBI¹²), $\lambda = 47.0257$ pm. The exposure time of each diffraction pattern was corrected for fluctuations and decay of the synchrotron beam by using monitor counts collected between the incident beam and the sample.

LaB_6 was used as an external standard for wavelength determination, zero shift, and 2θ correction. No correction for the difference between the actual and the set point temperature of the furnace and the cryostat was applied. Thus, the set point temperature is given throughout the whole paper. Samples were measured in capillaries (\varnothing 0.3 mm) made from Lindemann glass (low temperatures) and quartz glass (high temperatures) sealed under argon. No internal standard was added. All diffractograms were analyzed using the STOE software Win XPOW.¹³ For the Rietveld refinements the GSAS software package was applied.¹⁴ To obtain a reliable trend of the lattice parameters the same sets of variables were used in the final Rietveld refinements of all diffractograms (for details see Table 2).

DTA/TG Investigations. Using a Netzsch STA 409C, 27.6 mg of EuC_2 were heated to 1000 °C (argon atmosphere, heating rate: 10 °C/min) and cooled to 150 °C (cooling rate: 10 °C/min). The instrument is placed in a glovebox (N_2 atmosphere).

Raman Spectroscopy. A powdered sample of EuC_2 was sealed in a glass capillary ($\varnothing = 1$ mm, Ar atmosphere). The Raman spectrum was recorded with a Bruker IFS 66v/S and an attached FRAU 106/S (Nd:YAG laser, $\lambda = 1064$ nm, 75–80 mW laser power).

¹⁵¹Eu Mössbauer Spectroscopy. The Mössbauer effect (ME) measurements were carried out at $T = 100$ and 4.2 K in a variable ⁴He cryostat using a 100 mCi ¹⁵¹SmF₃ source. Mössbauer absorber samples, ~ 10 mg/cm², were prepared in a special sealed indium container under a clean Ar atmosphere. During measurements the source and absorber were kept at the same temperature.

Magnetic Susceptibilities. A polycrystalline sample of EuC_2 (weighed portion 21.23 mg) was sealed in a quartz capillary (Suprasil, Ar atmosphere). The magnetic susceptibilities were determined with a SQUID magnetometer (MPMS-5S, Quantum Design) in the temperature range 2–300 K at magnetic fields of $B_0 = 0.01, 0.05, 0.1,$ and 0.5 T. The diamagnetic correction of Eu^{2+} and C_2^{2-} was calculated to $\chi_m^{\text{dia}} = -46 \times 10^{-11} \text{ m}^3 \text{ mol}^{-1}$ (SI units).^{15,16}

Electrical Conductivity. A larger polycrystalline piece of EuC_2 of irregular shape was sanded to a nearly rectangular shape of typical dimensions of approximately $2 \times 1 \times 0.5 \text{ mm}^3$. The resistivity was measured by a standard DC four-probe technique in the temperature range from 6 to 300 K and in magnetic fields up to 14 T using a ⁴He magnet cryostat. The performing of the sample was performed in a glovebox (Ar atmosphere), whereas the measurements were carried out under vacuum conditions.

Results

Due to the different results^{8,9,11} given for the crystal structure of EuC_2 , our first aim was to solve this open question. The diffraction pattern obtained for our EuC_2 sample of high purity could not be indexed with a tetragonal unit cell as given in ref 8 and 11. However, the complex pattern could be indexed with a C-centered monoclinic unit cell and the lattice parameters $a \approx 701$ pm, $b \approx 442$ pm, $c \approx 759$ pm, and $\beta \approx 106.9^\circ$.¹⁷ These lattice parameters are very similar to those obtained for the low temperature modification of SrC_2 ($a \approx 705$ pm, $b \approx 447$ pm, $c \approx 768$ pm, and $\beta \approx 107.2^\circ$),¹⁸ which crystallizes in the ThC_2 type structure.¹⁹

(13) Win XPOW, version 1.04 (07-Jan-1999); Stoe & Cie GmbH: Darmstadt, Germany.

(14) Larson, A. C.; v. Dreele, R. B. *Los Alamos Laboratory, Rep. No. LA-UR-86-748*, 1987.

(15) Haberditzl, W. *Angew. Chem.* 1966, 78, 277–288.

(16) Lueken, H. *Magnetochemie*; Teubner: Stuttgart, Germany, 1999.

(17) Boulif, A.; Louer, D. J. *Appl. Crystallogr.* 1991, 24, 987–993.

(18) Vohn, V.; Knapp, M.; Ruschewitz, U. *J. Solid State Chem.* 2000, 151, 111–116.

(19) Hunt, E. B.; Rundle, R. E. *J. Am. Chem. Soc.* 1951, 73, 4777–4781.

(11) Sakai, T.; Adachi, G.; Yoshida, T.; Ueno, S.; Shiokawa, J. *Bull. Chem. Soc. Jpn.* 1982, 55, 699–703.

(12) Knapp, M.; Joco, V.; Baetz, C.; Brecht, H. H.; Berghaeuser, A.; Ehrenberg, H.; von Seggern, H.; Fuess, H. *Nucl. Instrum. Methods Phys. Res., Sect. A* 2004, 521, 565–570. Knapp, M.; Baetz, C.; Ehrenberg, H.; Fuess, H. *J. Synchrotron Radiat.* 2004, 11, 328–334.

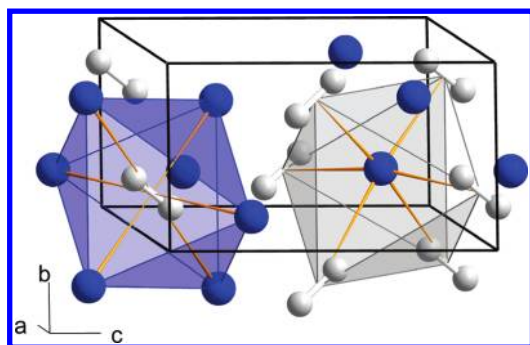
Table 1. Selected Structural Data of Modifications of EuC_2

	$\text{EuC}_2\text{-I}$	$\text{EuC}_2\text{-II}$	$\text{EuC}_2\text{-III}$
T/K	298	638	648
Space group, Z	$C2/c$, 4	$I4/mmm$, 2	$Fm\bar{3}m$, 4
Unit cell	$a = 700.54(2)$ pm $b = 441.85(1)$ pm $c = 758.71(2)$ pm $\beta = 106.887(2)^\circ$ $V = 0.22421(1)$ nm ³	$a = 414.94(1)$ pm $c = 662.61(3)$ pm $V = 0.11408(1)$ nm ³	$a = 613.78(3)$ pm $V = 0.23123(4)$ nm ³
Atomic coordinates	Eu 4e 0 0.1839(2) 1/4 C 8f 0.274(3) 0.182(3) 0.042(1)	Eu 2a 0 0 0 C 4e 0 0 0.441(2)	Eu 4a 0 0 0 C ^a 4b $1/2$ $1/2$ $1/2$
Distances (pm): Eu–C	281.8(1) 2x 288.9(1) 2x 290.0(2) 2x 296.0(2) 2x 313.1(1) 2x	292.7(15) 2x 296.0(2) 8x	
C–C	119.7(1)	116.9(1)	

^aDisordered C_2 dumbbell (occ. = 2).

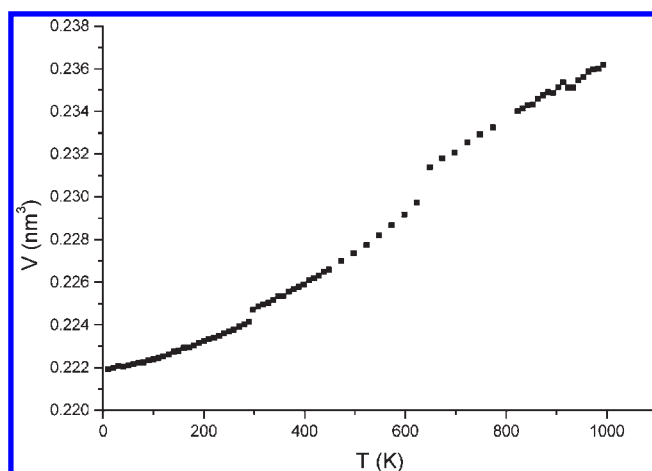
Table 2. Details of X-ray Powder Investigations on EuC_2 at 298 K (Synchrotron Radiation, $\lambda = 49.9604$ pm, Powder Diffractometer at Beamline B2, OBI Detector, Capillary: $\varnothing = 0.3$ mm, HasyLab, Hamburg/Germany)

Data range	$6.0^\circ \leq 2\theta \leq 35^\circ$, 7251 data points
Bragg reflections	204
Refined parameters	32 (including 20 background parameters)
Profile function	Modified Pseudo-Voigt ^{21,22}
Background	Linear interpolation function
R_p ; wR_p ; R_B	0.0476; 0.0625; 0.0814
Software for refinement	GSAS ¹⁴

**Figure 1.** Crystal structure of EuC_2 at room temperature ($C2/c$, $Z = 4$, ThC_2 type structure): Eu, blue balls; C, white balls.

Rietveld refinements confirm that EuC_2 also crystallizes in the ThC_2 type structure. Some structural details are given in Table 1 ($\text{EuC}_2\text{-I}$); details of the Rietveld refinement are summarized in Table 2.

A view of the crystal structure of EuC_2 is shown in Figure 1. Eu cations form a distorted fcc arrangement with C_2 dumbbells occupying octahedral holes in the metal lattice. The same arrangement is found in tetragonal CaC_2 . Here all C_2 dumbbells are aligned along the c axis and point toward the opposite corners of the Ca_6 octahedra, which are elongated in this direction. In EuC_2 , however, the C_2 dumbbells are tilted, no longer pointing toward the corners, but toward opposite trigonal faces of the Eu_6 octahedra. Each Eu cation is coordinated by ten carbon atoms of six C_2 dumbbells (see Figure 1). Four of these dumbbells coordinate side-on, and two end-on. This is similar to tetragonal CaC_2 , but here the end-on coordinating C_2 dumbbells are at opposite corners of the surrounding polyhedron; in EuC_2 they are next to each

**Figure 2.** Unit-cell volume of EuC_2 as function of temperature; standard deviations are in the range of the symbol size. The step in the volume curve at approximately 300 K is an artifact due to a change of equipment (cryostat to furnace); no internal standard was used for correction.

other (see Figure 1). Eu–C distances are given in Table 1, second column. The C–C distance obtained in a free refinement of all positional parameters is in good agreement with the typical distances for a C–C triple bond (120 pm).²⁰ This is already a first indicator that EuC_2 is best described with divalent Eu(II) according to $\text{Eu}^{2+}(\text{C}_2^{2-})$.

Temperature dependent synchrotron powder investigations reveal that EuC_2 crystallizes in the ThC_2 type structure in a wide temperature range from 10 K up to approximately 630 K. Only in a very small temperature window of ~ 638 K is the tetragonal CaC_2 type structure ($I4/mmm$, $Z = 2$) found; above 648 K cubic high temperature EuC_2 ($Fm\bar{3}m$, $Z = 4$) is observed. Structural details of these modifications are given in columns 3 and 4 of Table 1. The crystal structure of the tetragonal modification described above has the reduced C–C distance of 116.9 pm due to an increased thermal vibration of the C_2 dumbbells perpendicular to the C–C axis. This effect is quite common for acetylides and other compounds with diatomic dumbbells. In the cubic high temperature modification the C_2 dumbbells are completely

(20) Pauling, L. *The Nature of the Chemical Bond*, 3rd ed.; Cornell University Press, Ithaca, NY, 1960; p 230.

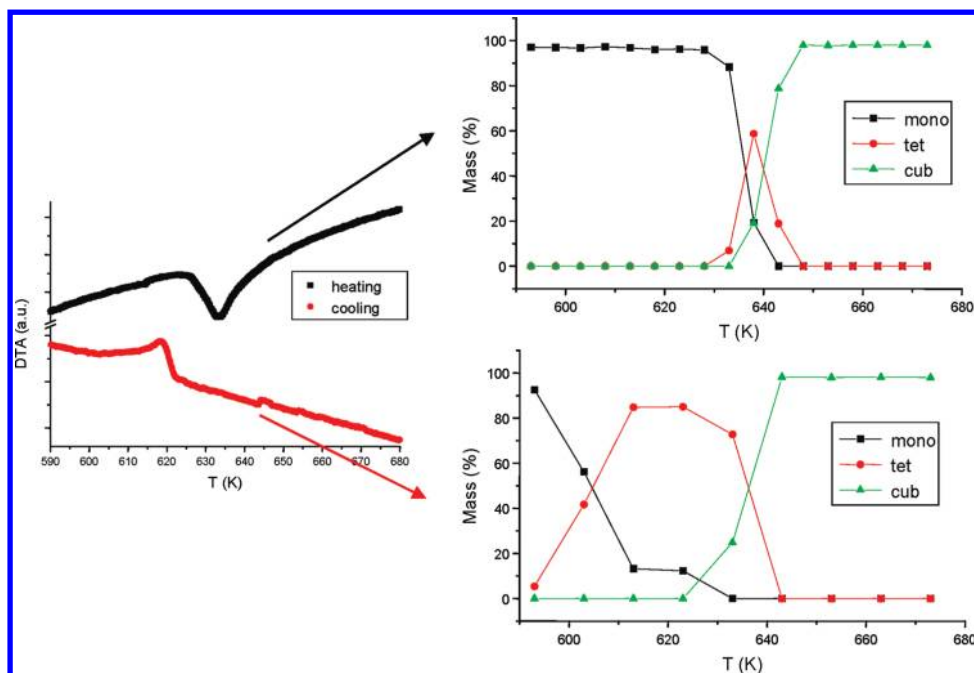


Figure 3. Phase transitions in EuC_2 : DTA (left) and phase compositions as obtained from Rietveld refinements of synchrotron powder diffraction data (right) upon heating (above) and cooling (below).

disordered. Their centers of gravity reside in the centers of the Eu_6 octahedra, which are no longer distorted so that a perfect NaCl type structure arrangement results.

In Figure 2 the unit-cell volume of EuC_2 as a function of temperature is shown as obtained from synchrotron powder diffraction data. The discontinuity around room temperature is an artifact due to the fact that two different measurement setups (low temperature/high temperature; see Experimental Section) have been used. No internal standard was added to correct the data. The discontinuity at approximately 648 K is due to a phase transition from low temperature EuC_2 to the cubic high temperature modification. The volume jump is indicative of a first-order transition, as also found for alkaline-earth metal acetylides AC_2 ($A = \text{Ca},^2 \text{Sr},^{18} \text{Ba}^{23}$). Throughout the whole temperature range a positive thermal expansion is found; i.e., no indications for a valence change from larger Eu(II)C_2 to smaller Eu(III)C_2 are observed.

In Figure 3 results of the DTA investigations are compared with those of the synchrotron powder experiments in a temperature range around the phase transition temperature. TG results are omitted as no significant effects were found. On the right-hand side of the figure a quantitative analysis of the diffraction data based on a Rietveld analysis is shown. The relative weight ratio of the different EuC_2 modifications is given. The results of both investigations are in good agreement. One signal is found in the DTA for the heating ($T_P \approx 635 \text{ K}$) and the cooling curve ($T_P \approx 620 \text{ K}$), both representing the transition from tetragonal to cubic EuC_2 and vice versa. A small hysteresis of $\Delta T_P \approx 15 \text{ K}$ is similar to those found for alkaline-earth metal acetylides.^{2,18,23} In none of our investigations on alkaline-earth metal acetylides we

Table 3. Experimental Frequencies $\tilde{\nu}(\text{C}\equiv\text{C})$ (cm^{-1}) of Selected Carbides of Composition MC_2

	$\tilde{\nu}(\text{C}\equiv\text{C})$ (cm^{-1})	ref
CaC_2 ($I4/mmm$, $Z = 2$)	1858	[2]
SrC_2 ($I4/mmm$, $Z = 2$)	1852	[18]
BaC_2 ($I4/mmm$, $Z = 2$)	1833	[23]
EuC_2 ($C2/c$, $Z = 4$)	1837	This work

have ever observed a signal for the transition from the monoclinic to the tetragonal modification. Thus, we assume that this transition occurs without a detectable evolution of heat. According to high-temperature synchrotron powder diffraction data a volume jump occurs at approximately 648 K upon heating. The slight differences to the DTA data ($T_P = 635 \text{ K}$) are probably due to the fact that the heating device of the powder diffractometer was not properly calibrated. The diffraction data also reveal that the stability range of tetragonal EuC_2 is very small upon heating. A temperature, where pure tetragonal EuC_2 exists, has not been found. However, upon cooling almost pure tetragonal EuC_2 was observed in the temperature 630–610 K. But below 600 K no detectable amounts of tetragonal EuC_2 were found. This is in disagreement with literature data.^{8,11} A possible explanation will be given below.

The synchrotron powder diffraction data already give a first indication that europium is in the divalent state in EuC_2 . To corroborate this assumption several other methods were used. Raman spectroscopy is an indirect probe, as it is very sensitive for the C–C stretching vibration. The C–C stretching vibration, which in turn is a very good indicator for the bonding situation in acetylides,²⁴ i.e. $\tilde{\nu}(\text{C}\equiv\text{C})$ in $\text{Eu}^{2+}(\text{C}_2^{2-})$, should differ significantly from $\tilde{\nu}(\text{C}\equiv\text{C})$ in $\text{Eu}^{3+}(\text{C}_2^{2-})(\text{e}^-)$. As the resulting wavenumber for $\tilde{\nu}(\text{C}\equiv\text{C})$ is very similar to those obtained for alkaline-earth metal carbides (see Table 3), it can be concluded that europium is

(21) Thompson, P.; Cox, D. E.; Hastings, J. B. *J. Appl. Crystallogr.* **1987**, *20*, 79–83.

(22) Finger, L. W.; Cox, D. E.; Jephcoat, A. P. *J. Appl. Crystallogr.* **1994**, *27*, 892–900.

(23) Vohn, V.; Kockelmann, W.; Ruschewitz, U. *J. Alloys Compd.* **1999**, *284*, 132–137.

(24) Ruschewitz, U. *Z. Anorg. Allg. Chem.* **2006**, *632*, 705–719.

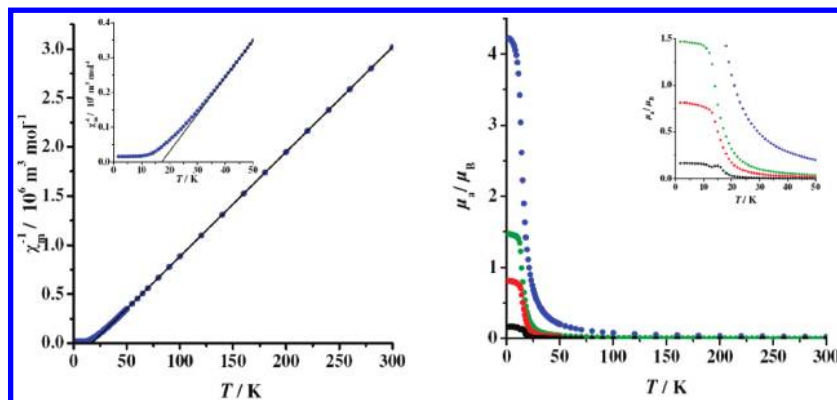


Figure 4. (a) EuC_2 : χ_m^{-1} - T diagram measured at 0.5 T; (blue) measured, (—) fit to Curie–Weiss law (40–300 K); the low temperature range is enlarged in the inset. (b) EuC_2 : μ_a - T diagram (μ_a : atomic magnetic dipole moment); (blue) 0.5, (green) 0.1, (red) 0.05, (black) 0.01 T; the low temperature range is enlarged in the inset.

probably divalent in EuC_2 , thereby confirming the results of the synchrotron powder diffraction data. For trivalent europium, i.e. $\text{Eu}^{3+}(\text{C}_2^{2-})(\text{e}^-)$, an expanded C–C is expected, which should lead to a weaker C–C bond and a significantly smaller wavenumber for the C–C stretching vibration.

In Figure 4a the results of magnetic susceptibility measurements vs temperature are shown plotted as χ_m^{-1} - T at $B_0 = 0.5$ T. No indications of EuO impurities are found at their $T_C = 69$ K. Above $T > 40$ K Curie–Weiss behavior is observed ($\chi_m = C/(T - \theta)$) with Weiss constant $\theta = 17.1$ K and Curie constant $C = 9.373 \times 10^{-5} \text{ m}^3 \text{ K mol}^{-1}$ corresponding to $\mu = 7.72 \mu_B$. This value is somewhat lower than the one expected for Eu^{2+} ($[4f^7]$, ground multiplet $^8\text{S}_{7/2}$, $\mu_{\text{eff}} = 7.9$)¹⁶ but differs strongly from the value expected for Eu^{3+} ($[4f^6]$, ground multiplet $^7\text{F}_0$, $\mu_{\text{eff}} = 3.5$ at 400 K).¹⁶ At $T < 40$ K, χ_m becomes field dependent. These results are indicative of ferromagnetic Eu–Eu interactions, as already described in the literature ($\mu = 8.04 \mu_B$, $\theta = 14$ K).¹¹ On the basis of μ_a vs T behavior (μ_a : atomic magnetic dipole moment) T_C was determined to 15 K (see Figure 4b), again in good agreement with literature data.¹¹

For a direct proof for the valence state of europium in EuC_2 at a microscopic level, ^{151}Eu Mössbauer spectra were recorded well above and below the ferromagnetic transition ($T_C = 15$ K; see Figure 5). For the measurement the sample from the resistivity measurements was crushed and ground to a fine powder. The ME spectrum in the paramagnetic state ($T = 100$ K) was analyzed with Lorentzian lines taking into account a quadrupole splitting. As evident from the figure, one mainly observes a narrow single line (line width: $\Gamma = 2.7(1)$ mm/s) with a value of the isomer shift (S) of $-11.92(3)$ mm/s, indicating that the valence state of the Eu in EuC_2 is indeed Eu^{2+} .²⁵ The single-line spectrum exhibits a small but finite value of the quadrupole splitting, $QS = 4.3(3)$ mm/s, which results from the noncubic local site symmetry around the Eu^{2+} ions in EuC_2 (see above). We also observe a minor component ($< 5\%$) with $S = 0.69(6)$ mm/s typical for Eu^{3+} (see arrow in Figure 5), which is obviously related to a tiny impurity phase due to a partial oxidation and/or hydrolysis of the powder sample during the preparation of the Mössbauer absorber. The amount of this minor impurity phase is found to be temperature independent. As

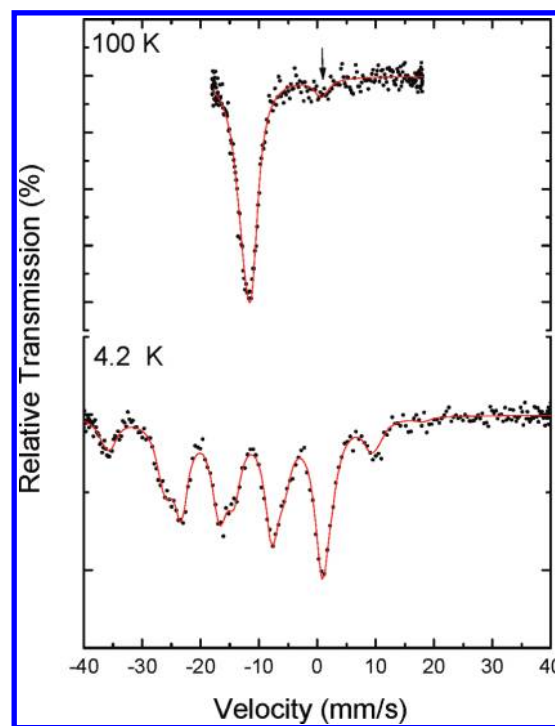


Figure 5. ^{151}Eu Mössbauer spectra of EuC_2 measured at 100 and 4.2 K. The arrow shows a minor impurity phase ($< 5\%$) of Eu^{3+} due to the oxidation of the absorber prepared for the Mössbauer measurements.

shown in Figure 5, the ME spectrum at 4.2 K displays a magnetic hyperfine (hf) splitting due to the magnetic ordering of the Eu^{2+} moments below T_C , which is consistent with our results obtained from magnetic susceptibility measurements. The value of the effective magnetic hf field (B_{eff}) at the Eu nucleus amounts to 31.41(8) T typical for magnetically ordered divalent Eu-based compounds. The absolute value of the isomer shift slightly decreases between 100 and 4.2 K ($S = -11.78(3)$ mm/s). This indicates a corresponding increase of the s-electron density at the Eu nucleus due to the temperature-induced decrease of the volume. Thus, the Mössbauer results provide a microscopic proof that the valence state of Eu in EuC_2 is in a stable Eu^{2+} state and corroborate the results of structural and Raman spectroscopic investigations as well as magnetic susceptibility measurements. The stability of Eu^{2+} in EuC_2 can easily be attributed to a half-filled 4f-shell.

(25) Bauminger, E. R.; Kalvius, G. M.; Nowik, I. *Mössbauer isomer shifts*; Shenoy, G. K., Wagner, F. E., Eds.; Amsterdam, The Netherlands, 1978; p 661.

In this respect, it is important to mention that Mössbauer measurements reported on previous EuC_2 samples¹⁰ revealed a very broad line width ($\Gamma = 6$ mm/s), which is nearly by a factor of 2 larger than that obtained for our sample. This reflects a considerable inhomogeneity of those samples. Moreover, the reported values of the shift, $S = -10.57(21)$ mm/s and $S = -10.70(20)$ mm/s, are much lower than those obtained for our samples, indicating a different electronic nature of the charge carriers. But it must be pointed out that the unit cells given for the samples under investigation ($a = 373$ pm, $c = 618$ pm) largely deviate from the unit cells found by us (see Table 1) and others ($a = 404.5$ pm, $c = 664.5$ pm).⁸ Therefore it can be excluded that the samples investigated in ref 10 are pure EuC_2 .

One unexpected result of the investigations by Adachi et al. was an increase in electrical resistivity with increasing temperature.¹¹ Such a behavior is typically observed for metallic compounds, but according to the results described above EuC_2 should be $\text{Eu}^{2+}(\text{C}_2)$ and semiconducting. Therefore, we also carried out measurements of the electrical conductivity of our high purity sample. Actually, for the conductivity measurements and the ¹⁵¹Eu Mössbauer spectroscopy the same sample was used, which was kept in gloveboxes with purified Ar atmospheres.

Sample handling and contacting the sintered polycrystalline piece of rectangular shape with copper wires were performed in a glovebox (Ar atmosphere) to prevent the sample from hydrolysis and oxidation. The transport to the cryostat and the measurement itself were carried out in vacuum conditions. The results of this measurement are shown in Figure 6.

The measurement recorded with no external magnetic field ($B_0 = 0$ T, black curve) shows a maximum at approximately 14 K, which is in agreement with $T_C = 15$ K as obtained from magnetic susceptibility measurements (see above). A similar behavior was obtained by Adachi et al. with a maximum at approximately 20 K in the resistivity vs temperature curve.¹¹ However, at temperatures above 20 K the literature data and our results differ, since we do not observe any increase of the electrical resistivity with increasing temperatures. According to our measurements EuC_2 is a semiconductor down to 15 K as expected from the divalent nature of europium. An intriguing result of our measurements is the CMR effect (colossal magnetoresistance), i.e. the enormous decrease of the electrical resistivity upon applying large magnetic fields up to $B_0 = 14$ T. This effect is most pronounced at the maximum of the curve at approximately 14 K. Applying a magnetic field $B_0 = 1$ T already decreases the electrical resistivity by a factor 10^3 . Adachi et al. found a similar, but a much less pronounced effect.¹¹ Measurements on different samples show that the resistivity strongly depends upon the quality of the respective sample: with improving purity and longer sintering the resistivity increases significantly above its Curie temperature and drops dramatically below.

All these observations show that high-purity samples and the best inert conditions possible are needed to measure the properties of air- and moisture-sensitive samples in a reliable way to accurately understand the compound's intrinsic behavior.

Discussion

In the last section we established that EuC_2 is a semiconducting carbide with europium in a divalent state. The

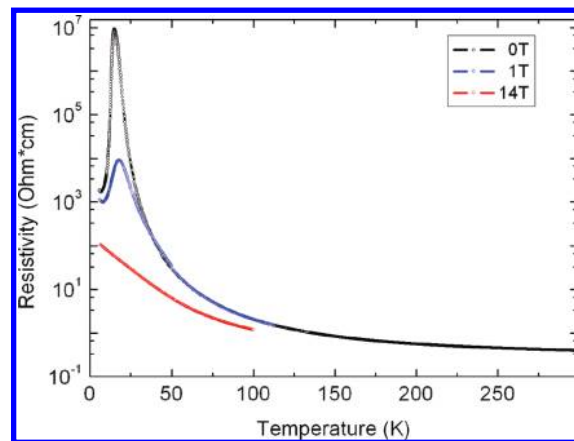


Figure 6. Electrical resistivity vs temperature of EuC_2 at various fields.

measurements show that a sample free of any impurities (EuO, etc.) could be synthesized. The literature controversy concerning the crystal structure of EuC_2 could be resolved: EuC_2 crystallizes in the monoclinic ThC_2 type structure. The tetragonal CaC_2 type structure was only found in a very small temperature range just below the transition to the cubic high temperature modification. But it is unclear why several authors reported a tetragonal modification at ambient conditions,^{8,11} which could not be repeated by others.⁹ Similar observations were made for CaC_2 . For many years a tetragonal modification was reported being stable at ambient conditions. But we could show that only impure CaC_2 samples (e.g., containing CaO) were found in this modification, whereas a pure single-phase sample crystallizes in the monoclinic ThC_2 type structure.² These impurities seem to hinder the phase transition from the tetragonal to the monoclinic modification of a freshly prepared sample upon cooling. Thus, the results on EuC_2 are very comparable to those of CaC_2 . It must be assumed that the samples synthesized in ref 8 and 11, which crystallize in the tetragonal modification, contained small amounts of impurities (e.g., EuO) probably not detectable with X-ray powder diffraction. The sample of ref 9 and our sample are, however, free of EuO impurities thereby crystallizing in the monoclinic modification.

Another important aspect, besides sample purity, is sample homogeneity. Is EuC_2 really a perfectly stoichiometric compound with composition $\text{Eu}_{1-x}\text{C}_2$ with $x = 0$? From XRPD data no hint of a nonstoichiometric behavior was found, as samples prepared from different Eu/C ratios always gave similar unit cells within standard deviations. This is corroborated by the small line widths obtained in the Mössbauer spectra. But our ongoing investigations in this field will try to clarify this aspect further.

In Figure 7 the unit-cell volumes per formula unit of most rare-earth metal carbides RE_2C_2 are presented. The unit-cell volumes decrease when going to the heavier rare-earth metals, as the radii of RE^{3+} contract in this direction. Two exceptions are found: EuC_2 and YbC_2 , both marked in red. In this work we showed that europium is divalent in EuC_2 thus explaining the larger size of its unit cell. But from Figure 7 it can be postulated that under pressure europium in EuC_2 should become trivalent and the resulting compound should be metallic. Actually, we found when pressing pellets from EuC_2 that the color of the pellets changes from black to silver metallic upon application of pressure. This effect is

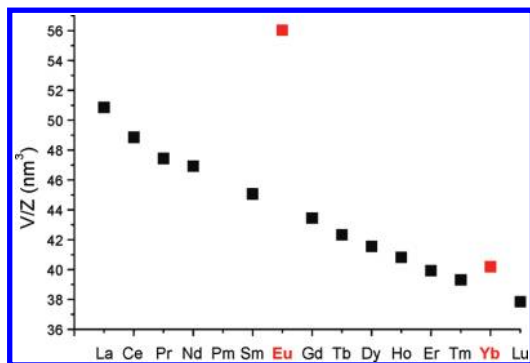


Figure 7. Unit-cell volumes per formula unit of rare-earth metal carbides $RE C_2$; data (with the exception of $Eu C_2$) were taken from the literature.

reversible. Measurements of the magnetic susceptibilities up to 10 kbar, however, did not show any significant effect.²⁶ Probably pressures higher than 10 kbar are needed for this transformation. Such experiments are also part of our current investigations.

In Figure 7 it can be seen that $Yb C_2$ also shows an increased unit-cell volume compared to neighboring rare-earth metal carbides $RE C_2$. But the effect is less pronounced than that for $Eu C_2$. Similar to divalent Eu in $Eu C_2$ (half-filled 4f-shell) this behavior can be attributed to a completely filled 4f-shell for divalent Yb, which seems, at least partly, to occur in $Yb C_2$. The synthesis and investigation of the structural and physical properties of $Yb C_2$ are another part of our studies in the field of rare-earth metal carbides. In Figure 8 the transition temperatures for the phase transition to a cubic high-temperature modification are given for several rare-earth and alkaline-earth metal carbides of composition MC_2 . Here is a clear distinction between those carbides with trivalent cations ($T_{PU} > 1400$ K) and those with divalent cations ($Ca C_2$, $Sr C_2$, $Ba C_2$, $Eu C_2$; $T_{PU} < 800$ K). $Yb C_2$ ($T_{PU} = 1023$ K)²⁶ is somewhere in-between, manifesting its exceptional position and making it a very interesting compound for further investigations.

In conclusion, we have shown that $Eu C_2$ crystallizes in the $Th C_2$ type structure at ambient conditions thus clarifying a controversy in the literature. The tetragonal $Ca C_2$ type

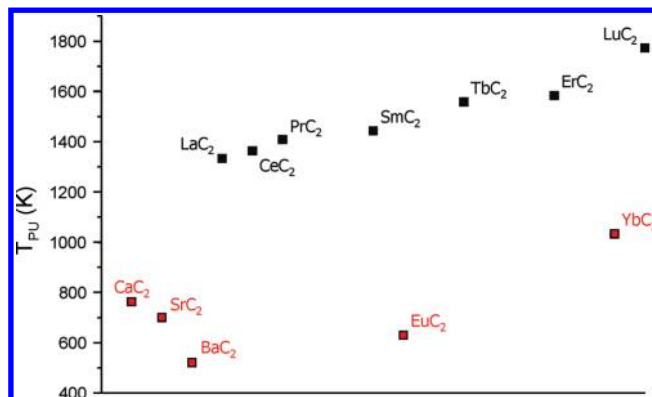


Figure 8. Transition temperatures of rare-earth and alkaline-earth metal carbides of composition MC_2 for a phase transition to a cubic high temperature modification. Red symbols represent results of our own work ($Ca C_2$,² $Sr C_2$,¹⁸ $Ba C_2$,²³ $Eu C_2$,^{thiswork} $Yb C_2$ ²⁶); black symbols are taken from the literature.

structure was only found in a very small temperature range just below the transition to a cubic high temperature modification ($T_{PU} = 648$ K). The stability of these different modifications depends very much on the purity of the samples. Only for very pure samples, free of any oxide impurities, the monoclinic $Th C_2$ type structure is found at ambient conditions. Mössbauer and Raman spectra as well as measurements of the magnetic susceptibilities reveal that europium is divalent in $Eu C_2$. Measurements of the electrical resistivity show a maximum at approximately 14 K, where a CMR effect (colossal magnetoresistance) was found. Above 14 K $Eu C_2$ is a typical magnetic semiconductor with a ferromagnetic Curie temperature of ca. 15 K. It was shown that these properties, especially the resistivity and the CMR effect, strongly depend upon the purity of the sample.

Acknowledgment. The help of Dr. Carsten Bächtz and Dr. Michael Knapp (synchrotron powder diffraction), Prof. Dr. Angela Möller (Raman spectroscopy), and Dr. Klaus Müller-Buschbaum (DTA/TG investigations) is greatly acknowledged. We would like to thank the German Research Foundation (DFG) for financial support (SPP 1166, SFB 608).

(26) Wandner, D. PhD Thesis, University of Cologne, Cologne, Germany, 2007.